ResearchGate

See discussions, stats, and author profiles for this publication at: https://www.researchgate.net/publication/255692532

Coupled Unimolecular Dissociation Kinetics of Bromotoluene Radical Cations

ARTICLE *in* THE JOURNAL OF PHYSICAL CHEMISTRY A · AUGUST 2013

Impact Factor: 2.69 · DOI: 10.1021/jp4031442 · Source: PubMed

CITATION
1

READS
26

3 AUTHORS, INCLUDING:

Seung Koo Shin
Pohang University of Science and Technology
79 PUBLICATIONS **1,346** CITATIONS

SEE PROFILE

Available from: Seung Koo Shin
Retrieved on: 22 January 2016

THE JOURNAL OF PHYSICAL CHEMISTRY A

Article

pubs.acs.org/JPCA

Coupled Unimolecular Dissociation Kinetics of Bromotoluene Radical Cations

Jongcheol Seo,[†] Seung-Joon Kim,[‡] and Seung Koo Shin*[,†]

[†]Department of Chemistry, Pohang University of Science and Technology, Pohang, Korea 789-784

[‡]Department of Chemistry, Hannam University, Daejeon, Korea 305-811

Supporting Information

ABSTRACT: The unimolecular dissociations of *o*-, *m*-, and *p*-bromotoluene radical cations to $C_7H_7^+$ (benzylium and tropylium) are examined by considering the coupling of the three isomers in the dissociation pathways. The potential energy surface obtained from ab initio calculations suggests the interconversion of isomers through methylene and hydrogen migrations on the ring. The rate equations for each isomer are combined together to form a rate matrix for coupled reactions. The rate matrix contains the microcanonical rate constants for all elementary steps, which are calculated using Rice−Ramsperger−Kassel−Marcus theory based on the molecular parameters obtained from density functional theory. The unimolecular dissociation rates for coupled reactions are determined by numerically solving the matrix equation. As a result of reaction coupling, the product branching ratio becomes time-dependent and the reaction rates of three isomers become parallel to one another as the energy increases, although their initial rates differently vary with energy. The calculated rate−energy curves fall below the time-resolved photodissociation data in the energy range 2.2−2.7 eV but are in line with the photoelectron photoion coincidence data in the energy range 2.7−3.5 eV. The discrepancy between experiment and theory in the low-energy region is ascribed to the uncertainties of the potential energy surface as well as the contribution of the radiative relaxation rate that has not been taken into account in the theoretical calculations. The rate−energy curves are then used to calculate the thermal reaction rate constants, and the Arrhenius parameters are determined in the temperature range 700−1300 K. Comparison of the activation energy and entropy obtained from the Arrhenius plot with the calculated enthalpy and entropy changes between the reactant and the highest-lying transition state suggests that a series of [1,2] H-atom migrations occurring near the entrance comprise the rate-determining steps and the subsequent [1,2] H-atom migrations play an important role in increasing the activation energy and decreasing the entropy by reducing the net flux to the exit.

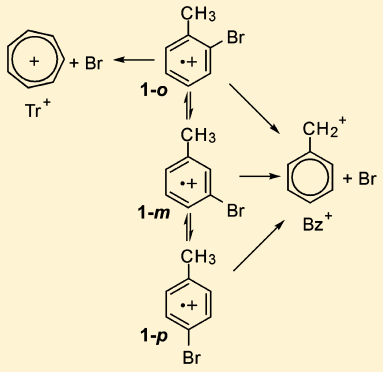

INTRODUCTION

The unimolecular dissociations of halotoluene radical cations to $C_7H_7^+$ (benzylium and tropylium) have been studied by both experiment[1−11] and theory[12−15] to find the major product channel and to determine the rate constant as a function of internal energy. However, both consensus and controversy exist regarding the mechanism of the unimolecular dissociation. The current consensus is that the reaction proceeds through two competing pathways, and the production of the benzylium ion (Bz^+) is predominant,[8−11,13−15] although the formation of the tropylium ion (Tr^+) is thermodynamically most stable.[16−18]

The controversy lies in whether the two product channels are split directly from a reactant or later on from a common intermediate and whether the unimolecular dissociations of *o*-, *m*-, and *p*-isomers are strongly coupled together or independent of one another. Previously, we studied the kinetics of competing multiple-barrier unimolecular dissociations of chlorotoluene radical cations without considering coupling on the basis of the potential energy surface calculated at the SCF level of theory.[12,14] Recently, Choe reported the potential energy surface of chloro-, bromo- and iodotoluene radical cations using density functional theory (DFT), which indicated the coupling of *o*-, *m*-, and *p*-isomers.[13,15] However, the steady-state approximation was used to evaluate the unimolecular dissociation rate constant for each isomer independent of one another. To address the controversy and to examine the effect of coupling on the reaction kinetics, we obtain the potential energy surface of bromotoluene radical cations with DFT and study the kinetics of the coupled unimolecular dissociations without resorting to the steady-state approximation.

Of the halotoluenes, bromotoluene is chosen because it is most well-characterized by experiment. The energy-selective dissociation rate constants were reported in the internal energy range 2.2−3.5 eV from time-resolved photodissociation (TRPD)[8,9] and photoelectron−photoion coincidence (PEPICO)[3] experiments. The structure of $C_7H_7^+$ was identified as the benzylium ion by ion−molecule reactions of the TRPD products in an ion cyclotron resonance cell.[8,9]

Special Issue: Curt Wittig Festschrift

Received: March 30, 2013
Revised: August 4, 2013
Published: August 5, 2013

ACS Publications © 2013 American Chemical Society

dx.doi.org/10.1021/jp4031442 | J. Phys. Chem. A 2013, 117, 11924−11932

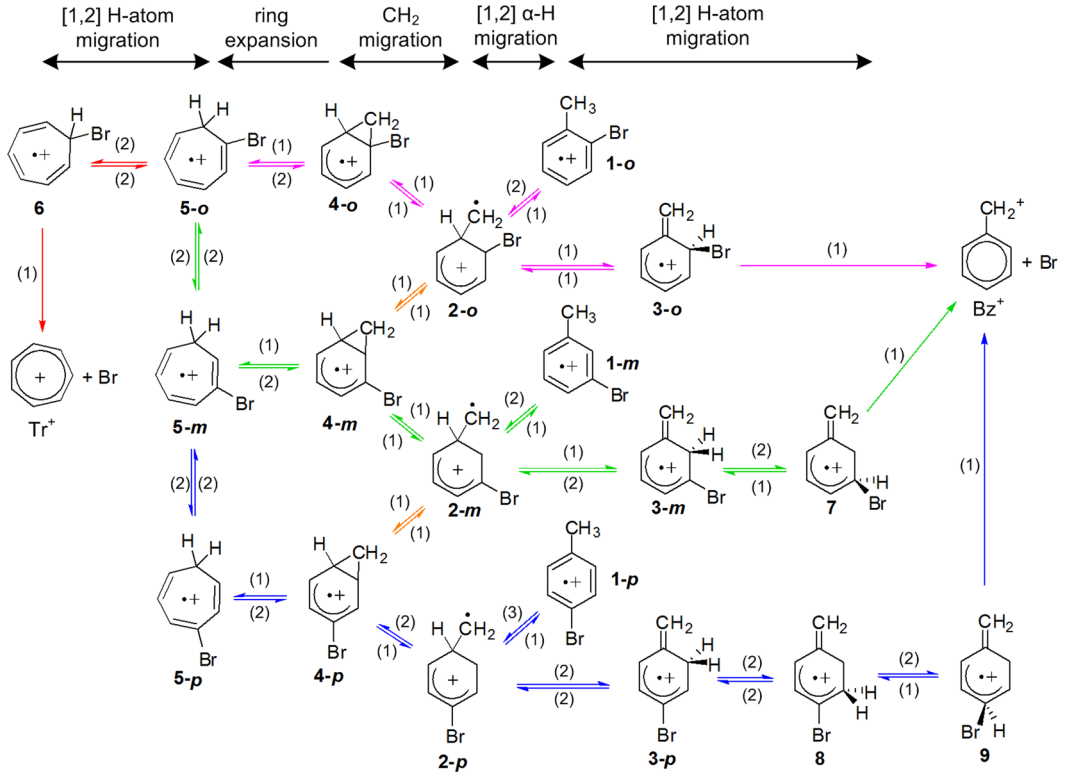

Figure 1. Mechanism of the unimolecular dissociation of the *o*-, *m*-, and *p*-bromotoluene radical cations denoted by **1**-*o*, **1**-*m*, and **1**-*p*, respectively. The benzylium ion (Bz^+) and the tropylium ion (Tr^+) are the bromine-loss products. The local minima found on the minimum-energy reaction paths are presented as reaction intermediates. The value in parentheses denotes the reaction degeneracy for each elementary process. The potential energy surfaces of the colored reaction paths are shown in Figure 2.

The mechanism considered in the present study is shown in Figure 1. Several rearrangement processes are involved here: [1,2] α-H migration from the reactant **1**-***x*** (x = *o*, *m*, *p*) to **2**-***x*** as the initial step, [1,2] H-atom migration or [1,2] CH_2 bridging from a common intermediate **2**-***x*** to **3**-***x*** toward Bz^+ or to **4**-***x*** toward Tr^+, respectively, as well as subsequent [1,2] H-atom migration on the ring in the benzylium channel or ring expansion in the tropylium channel. In addition, CH_2 migration between **2**-*o* and **2**-*m* via **4**-*m* as well as that between **2**-*m* and **2**-*p* via **4**-*p* are included in the mechanism to account for the coupling of the three isomers. Moreover, [1,2] H-atom migration on the seven-membered ring between adjacent **5**-***x***'s is also considered for the coupling. Thus, there are three reactants, 16 intermediates and 24 transition states participating in the coupled unimolecular dissociation reaction.

The microcanonical rate constant is calculated for each elementary step using Rice–Ramsperger–Kassel–Marcus (RRKM) theory and the rate-constant matrix is constructed for the coupled differential rate equations by using three reactants and 16 intermediates as the basis for the matrix. Then the 19 × 19 matrix equation is numerically solved for each isomer. Temporal variations of all transient species are examined to identify most abundant species in the reaction and to extract the rate constant for the coupled reaction. The resulting rate–energy curve is plotted for each of the isomers to compare with the TRPD and PEPICO data. Finally, we convert the unimolecular dissociation rate constant to the thermal rate constant in the temperature range 700–1300 K and determine Arrhenius parameters for coupled unimolecular dissociations of the bromotoluene radical cations. The activation energy and entropy obtained from the Arrhenius plot are compared with the enthalpy and entropy changes calculated from partition functions to examine the effects of the coupled multiple-barrier processes on the overall dissociation kinetics.

CALCULATIONAL DETAIL

The geometries and relative energies of the reactants, the products, the local minima, and the transition states along the dissociation pathways of bromotoluene radical cations were calculated using DFT with the Becke three-parameter Lee–Yang–Parr (B3LYP) functional and the augmented correlation-consistent polarized valence-only double-ζ (aug-cc-pVDZ) basis set. A transition state was searched between the local minima using a synchronous transit-guided quasi-Newton method.[19] Harmonic vibrational frequencies were obtained at the same level of theory and used in the RRKM calculations after scaling by 0.97.[20] All calculations were carried out using a Gaussian-03 program.[21] Molecular parameters, such as the relative energies, the vibrational frequencies, and the rotational constants of the reactants, the products, and all transient species are given in Tables S1 and S2 (Supporting Information).

The RRKM calculation was carried out by using a homemade program. The RRKM rate constant for a unimolecular reaction involving a single elementary step is given by eq 1.[22]

$$k(E) = \frac{\sigma W^{\ddagger}(E - E_0 - E_r^{\ddagger})}{h\rho(E - E_r)} \quad (1)$$

E is the internal energy of an ion, σ is the reaction degeneracy, $W^{\ddagger}$ is the sum of vibrational states in an activated transition state, h is Planck's constant, and ρ is the density of vibrational

dx.doi.org/10.1021/jp4031442 | J. Phys. Chem. A 2013, 117, 11924–11932

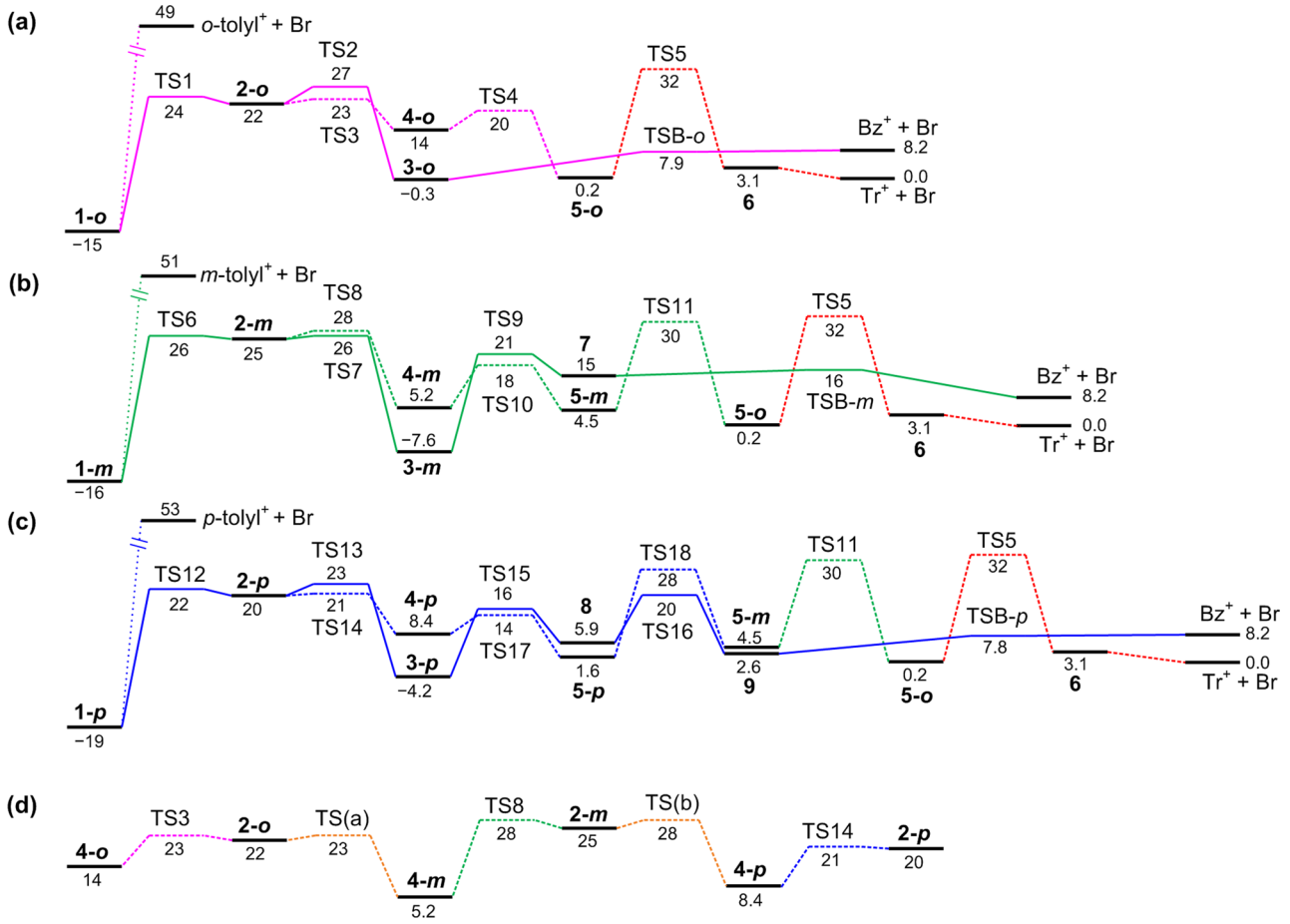

Figure 2. Minimum-energy path from the (a) *o*-, (b) *m*-, and (c) *p*-bromotoluene radical cations to $C_7H_7^+$ (Bz^+ and Tr^+). The dissociation limits to the *o*-, *m*-, and *p*-tolylium ion plus bromine are denoted by *o*-, *m*-, and *p*-tolyl$^+$ + Br. (d) Minimum-energy path that couples the *o*-, *m*-, and *p*-isomers. Each energy level is relative to Tr^+ plus bromine and corrected for the zero-point energy. Energies are given in units of kcal mol^{-1}.

states of the reactant. E_0 is the energy of the transition state relative to the reactant corrected for the zero-point vibrational energy. $E_r^{\ddagger}$ and E_r denote the adiabatic rotational energies of the transition state and the reactant, which are subtracted from the internal energy. The adiabatic rotational energy of the reactant is assumed to be $E_r = 3k_BT/2$. We also assume that the angular momentum of overall rotation is conserved during the reaction. Thus, the adiabatic rotational energy of the transition state is obtained by considering the moment of inertia as given in eq 2.[22]

$$E_r^{\ddagger} = E_r\left(\frac{I}{I^{\ddagger}}\right) = \frac{3k_BT}{2}\left(\frac{I}{I^{\ddagger}}\right) \quad (2)$$

I and $I^{\ddagger}$ represent the moment of inertia of the reactant and the transition state. The adiabatic rotational energies of other transient species along the dissociation pathways are similarly obtained. Thus, $W^{\ddagger}(E - E_0 - E_r^{\ddagger})$ is the sum of states of the activated transition state with an internal energy of $E - E_0 - E_r^{\ddagger}$ and $\rho(E - E_r)$ is the density of states of the reactant with an internal energy of $E - E_r$. Each normal mode of vibration as well as the internal rotation of the methyl group is treated as a harmonic oscillator. The density and sum of states were calculated using a Beyer−Swinehart direct counting algorithm.[22]

For each elementary step shown in Figure 1, the microcanonical rate constant was calculated at various temperatures using eq 1 in the internal energy range 15 000−60 000 cm^{-1} at every 1 cm^{-1} step. At a given internal energy E, the overall dissociation rate constant was then determined by solving a matrix equation[14] composed of a full set of coupled, linear first-order differential rate equations for three reactants and 16 intermediates. The 19 × 19 matrix equation filled with RRKM rate constants was numerically solved using a MATLAB program (see the Supporting Information). Populations of the reactant and intermediates were calculated at 10 000 time points from time zero to the time when the sum of all reactant and intermediate populations reached 1 ppm. The decay of total $C_7H_7Br^{+\bullet}$ populations obtained from the sum of the reactant and all intermediates was fit to a multiple exponential function as given in eq 3.

$$f(t) = c_1 \exp^{-t/\tau_1} + c_2 \exp^{-t/\tau_2} + c_3 \exp^{-t/\tau_3} \quad (3)$$

c_n and τ_n (n = 1, 2, 3) denote the amplitude and decay time constant, respectively. The inverse of the effective decay time constant ($\tau_{eff} = c_1\tau_1 + c_2\tau_2 + c_3\tau_3$) results in the microcanonical rate constant for the overall reaction at the internal energy E, as written in eq 4.

$$k_{uni}(E) = \frac{1}{\tau_{eff}(E)} \quad (4)$$

The canonical rate constant at constant temperature was calculated by convoluting $k_{uni}(E) = 1/\tau_{eff}(E)$ with the Boltzmann distribution of the internal energy $P(E)$, as given in eqs 5−7.[23]

dx.doi.org/10.1021/jp4031442 | J. Phys. Chem. A 2013, 117, 11924−11932

$$k(T) = \int_0^\infty k_{uni}(E)\,P(E)\,dE \quad (5)$$

$$P(E) = \frac{\rho(E)\,\exp(-E/k_BT)}{Q_V} \quad (6)$$

$$Q_V = \sum \rho(E)\,\exp(-E/k_BT) \quad (7)$$

$P(E)$ is the probability of finding a reactant at the internal energy E, and Q_V is the canonical partition function for the vibrational degrees of freedom.

The populations of the two products were calculated at 10^6 time points until their sum reached 0.999. Because the benzylium ion is produced through three different exit channels: **3-*o*** → Bz^+, **7** → Bz^+, and **9** → Bz^+, the total benzylium population is obtained from the sum of the products from all three exit channels. In contrast, the tropylium population is obtained from the depletion of **6** through a single exit channel, **6** → Tr^+.

RESULTS

The minimum-energy paths from the *o*-, *m*-, and *p*-bromotoluene radical cations **1-*x*** (*x* = *o*, *m*, *p*) to Bz^+ and Tr^+ are shown in Figure 2a–c. The dissociation limits to the *o*-, *m*-, and *p*-tolylium ions (tolyl$^+$) plus bromine are also depicted in Figure 2a–c. The energy levels of the reactants decrease in the order **1-*o*** > **1-*m*** > **1-*p***. The *o*-, *m*-, and *p*-tolylium ions plus bromine are 64, 67, and 67 kcal mol^{-1} higher in energy than **1-*o***, **1-*m***, and **1-*p***, respectively. In the internal energy range 2.0–3.6 eV, the direct dissociation to the tolylium ion is considered to be negligible because it requires energy greater than 2.8–3.0 eV. Thus, we focus on the unimolecular dissociations to the benzylium and tropylium ions. The first step involves a [1,2] α-H migration from **1-*x*** to **2-*x*** with a barrier of 39, 42, and 41 kcal mol^{-1} for *x* = *o*, *m*, and *p*, respectively. Of the intermediates along the dissociation pathways, **2-*x*** is least stable and the reverse barrier to **1-*x*** is very low in the range 1–2 kcal mol^{-1}. At the second step, the reaction is divided into two competing pathways, the [1,2] H-atom migration from **2-*x*** to **3-*x*** toward Bz^+ and the CH_2 bridging from **2-*x*** to **4-*x*** toward Tr^+. Their barriers are also low, 1–5 kcal mol^{-1} for the [1,2] H-atom migration and 1–3 kcal mol^{-1} for the CH_2 bridging. For each isomer, **3-*x*** is the most stable intermediate. Notably, the energy level of **3-*x*** decreases in order, **3-*o*** > **3-*p*** > **3-*m***, which manifests both the electron-donating resonance effect that stabilizes **3-*m*** and the electron-withdrawing inductive effect that destabilizes **3-*o*** and **3-*p***.

The benzylium channel starting from **3-*x*** proceeds to the exit in one step (**3-*o*** → Bz^+) or in two steps (**3-*m*** → **7** → Bz^+) or in three steps (**3-*p*** → **8** → **9** → Bz^+). Multistep processes involve [1,2] H-atom migrations on the six-membered ring prior to C–Br cleavage. The barrier for this H-atom migration is high, 29 kcal mol^{-1} for **3-*m*** → **7**, and 20 and 14 kcal mol^{-1} for **3-*p*** → **8** and **8** → **9**, respectively. On the other hand, the tropylium channel starting from **4-*x*** proceeds through a ring expansion followed by a series of [1,2] H-atom migrations on the seven-membered ring prior to C–Br cleavage. The ring expansion (**4-*x*** → **5-*x***) occurs with a barrier of 6, 13, and 6 kcal mol^{-1} for *x* = *o*, *m*, and *p*, respectively. The [1,2] H-atom migration on the seven-membered ring has a high barrier: 32 kcal mol^{-1} for **5-*o*** → **6**, 26 kcal mol^{-1} for **5-*m*** → **5-*o***, and 26 kcal mol^{-1} for **5-*p*** → **5-*m***. Importantly, [1,2] H-atom migrations between **5-*o*** and **5-*m*** and between **5-*m*** and **5-*p*** conjoin the three isomers. Three **4-*x*** intermediates can also interconnect the three isomers prior to ring expansion through CH_2 migrations between **2-*m*** and **2-*o*** and between **2-*p*** and **2-*m***, as shown in Figure 2d. These CH_2 migrations take place with a barrier of 9–23 kcal mol^{-1}, which is lower than the barrier for the coupling [1,2] H-atom migration. Thus, the CH_2 migration path shown in Figure 2d is considered as the minimum-energy, least-action path that couples the *o*-, *m*-, and *p*-isomers.

The final step to Bz^+ involves C–Br cleavage with a product-like transition state and the barrier height is in the range 1.3–8.2 kcal mol^{-1}. On the contrary, the C–Br cleavage to Tr^+ exhibits no transition state between **6** and the product at the B3LYP level. The highest barrier for the benzylium channel is located at TS2, TS7, and TS13, between **2-*x*** and **3-*x***, and the barrier height is 42 kcal mol^{-1} for the three isomers. The highest barrier for the tropylium channel is located at TS5 near the exit, between **5-*o*** and **6**, and the height is 47, 48, and 51 kcal mol^{-1} for the *o*-, *m*-, and *p*-isomers, respectively. Taken together, the potential energy surface shown in Figure 2 suggests that the benzylium channel involves fewer barriers than the tropylium channel and the three isomers are coupled together through CH_2 migrations on the six-membered ring prior to ring expansion as well as through [1,2] H-atom migrations on the seven-membered ring after ring expansion.

Figure 3 shows temporal variations of the relative abundances of **1-*x*** (*x* = *o*, *m*, *p*), $C_7H_7Br^+$ (the sum of the reactant and all intermediates), and the products as well as the product branching ratio obtained from the unimolecular dissociations of the *o*-, *m*-, *p*-bromotoluene radical cations having an internal energy of 2.8 eV at 298 K. In Figure 3a, the decay of $C_7H_7Br^{+\bullet}$ is presented along with temporal variations of the transient **1-*x*** species. The decay of $C_7H_7Br^{+\bullet}$ population from *o*-, *m*-, and *p*-isomers was fit to bi-, single-, and triple-exponentials with the effective decay time constant (τ_{eff}) of 12.7, 25.4, and 17.4 μs, respectively. The reciprocal of τ_{eff} was used as the overall microcanonical rate constant for each isomer. The fit parameters are listed in Table S3 of the Supporting Information.

In the case of the *o*-isomer, **1-*o*** decays with three time constants (3.7, 8.5, and 18.7 μs). The decay of **1-*o*** is not single exponential because both **1-*m*** and **1-*p*** are coupled to **1-*o*** through the CH_2 migration as well as the [1,2] H-atom migration. In contrast, **1-*m*** rises with the time constant of τ_{rise} = 8.7 μs and then falls with the time constant of τ_{fall} = 18.9 μs, and **1-*p*** ascends with τ_{rise} = 3.7 μs and then descends with two time constants, τ_{fall} = 8.8 and 18.9 μs. The first decay time constant (3.7 μs) for **1-*o*** is identical to τ_{rise} of **1-*p***, whereas the second decay time constant (8.5 μs) for **1-*o*** is nearly identical to τ_{rise} of **1-*m*** and equal to the first τ_{fall} for **1-*p***. The third decay time constant (18.7 μs) for **1-*o*** is almost identical to both τ_{fall} of **1-*m*** and the second τ_{fall} for **1-*p***. The rise and fall of **1-*m*** and **1-*p*** are closely correlated with the decay of **1-*o***, demonstrating the effect of coupling on the overall reaction kinetics. Although **1-*o*** decays with the effective time constant of τ_{eff} = 9.3 μs, total $C_7H_7Br^{+\bullet}$ descends more slowly with τ_{eff} = 12.7 μs. Apparently, the coupling of **1-*o*** with **1-*m*** and **1-*p*** slows down the overall dissociation rate.

For the *m*-isomer, while **1-*m*** decays with three constants of 4.7, 11.0, and 24.2 μs, **1-*o*** rises with τ_{rise} = 12.7 μs and then falls with τ_{fall} = 13.5 and 24.9 μs, and **1-*p*** ascends with τ_{rise} = 5.6 μs and descends with τ_{fall} = 5.6 and 25.3 μs. The coupling of **1-*m*** with **1-*o*** and **1-*p*** induces the rise of **1-*o*** and **1-*p***, and then all three **1-*x*** species decay slowly with a nearly identical time

dx.doi.org/10.1021/jp4031442 | J. Phys. Chem. A 2013, 117, 11924–11932

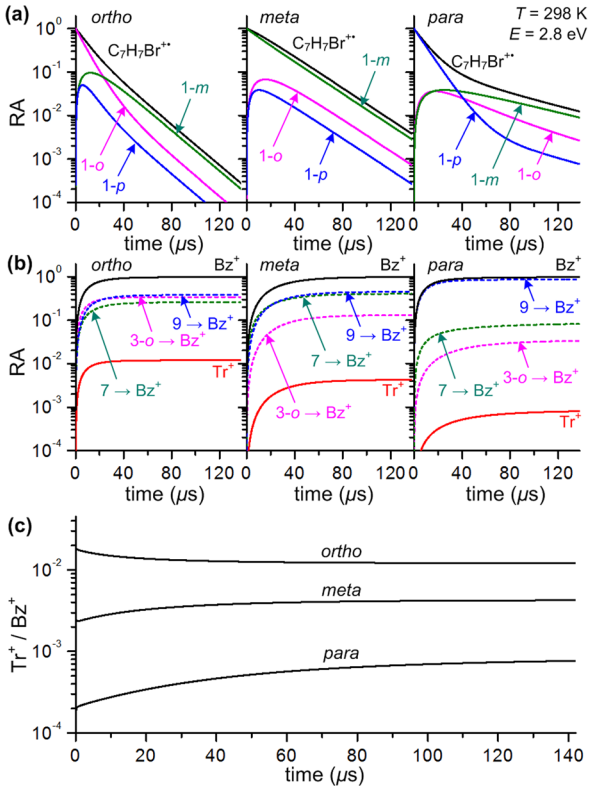

Figure 3. Temporal variations of (a) the relative abundance (RA) of $C_7H_7Br^{+\bullet}$, (b) the RAs of the products (Bz^+ and Tr^+), and (c) the product branching ratio (Tr^+/Bz^+). All three *o*-, *m*-, and *p*-bromotoluene radical cations have the same internal energy of 2.8 eV at 298 K. $C_7H_7Br^{+\bullet}$ (black) represents the sum of the reactant and all intermediates formed prior to C−Br cleavage. **1-*o*** (magenta), **1-*m*** (green), and **1-*p*** (blue) denote the initial reactant as well as the transient species. Bz^+ (black), Tr^+ (red), and Bz^+ produced through three exit channels, **3-*o*** → Bz^+ (magenta dash), **7** → Bz^+ (green dash), and **9** → Bz^+ (blue dash). The product branching ratio refers to Tr^+ (red)/Bz^+ (black).

constant of 24.2−25.3 μs after an induction period. Thus, the decay rate of $C_7H_7Br^{+\bullet}$ (τ_{eff} = 25.4 μs) is slightly slower than that of **1-*m*** (τ_{eff} = 24.0 μs).

In the case of the *p*-isomer, **1-*p*** is depleted with time constants of 9.7, 25.9, and 61.2 μs (τ_{eff} = 10.2 μs). In constrast, **1-*o*** and **1-*m*** rise with τ_{rise} = 10.7 and 12.6 μs, respectively, and then **1-*o*** descends with τ_{fall} = 27.1 and 64.6 μs and **1-*m*** falls with τ_{fall} = 69.1 μs. Similarly to the *o*- and *m*-isomers, the coupling of **1-*p*** with **1-*o*** and **1-*m*** significantly slows down the overall decay rate from τ_{eff} = 10.2 μs for **1-*p*** to τ_{eff} = 17.4 μs for $C_7H_7Br^{+\bullet}$.

Figure 3b presents temporal variations of the products (Bz^+ and Tr^+) coming out of four exit channels: three channels (**3-*o*** → Bz^+, **7** → Bz^+, **9** → Bz^+) for the benzylium ion and one channel (**6** → Tr^+) for the tropylium ion. The rise of total Bz^+ is also plotted in Figure 3b. To quantify the data, we analyze the product yields at an arbitrary time point of $5\tau_{eff}$. At $5\tau_{eff}$ of 63.5, 127.0, and 87.0 μs for the *o*-, *m*-, and *p*-isomer, respectively, yields of Bz^+ and Tr^+ are 0.971 and 0.012 from the *o*-isomer, 0.988 and 0.004 from the *m*-isomer, and 0.969 and 0.001 from the *p*-isomer, respectively. The benzylium ion is predominant in all three isomers. The three exit channels, **3-*o*** → Bz^+, **7** → Bz^+, and **9**→ Bz^+, contribute to the total production of Bz^+ as follows: 35%, 26%, and 39% for the *o*-isomer; 13%, 41%, and 46% for the *m*-isomer; 3%, 8%, and 89% for the *p*-isomer, respectively. Thus, the coupling significantly alters the dissociation pathways for each isomer and the para exit channel going through **9** → Bz^+ is favored over the other two exit channels in all three isomers. To compare the slope of the product appearance, we normalize the relative abundance of the product from each channel with its long-time limit (see Figure S1 of the Supporting Information). Notably, the rise of the tropylium ion from **6** → Tr^+ coincides with the rise of the benzylium ion from **3-*o*** → Bz^+ in all three isomers. The fact that the two different product channels have the same rise time suggests that they are derived from a common precursor, which is **2-*o***. Thus, for all three isomers having an internal energy of 2.8 eV at 298 K, the tropylium ion is produced via the same precursor **2-*o*** formed through the minimum-energy coupling pathway shown in Figure 2d.

Figure 3c exhibits the temporal variations of the product branching ratio (Tr^+/Bz^+) obtained from the three isomers. The product branching ratio varies with time because of the coupling and reaches a steady state after some induction periods. The yield of Tr^+ decreases in the order ortho > meta > para, as the yield of Bz^+ increases in the order ortho > meta > para.

Taking these results together, the overall dissociation process can be simplified as shown in Scheme 1: All three isomers are coupled to one another and dissociate to the benzylium ion through all three exit channels, but they yield the tropylium ion only through the ortho channel.

Scheme 1. Simplified Reaction Scheme for the Coupled Unimolecular Dissociations of the Bromotoluene Radical Cations

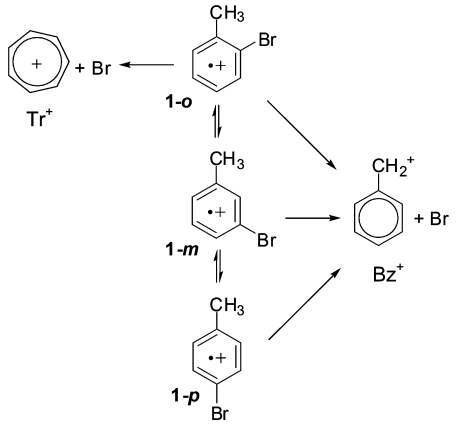

Figure 4 displays the rate−energy curves for the coupled unimolecular dissociations of *o*-, *m*-, *p*-bromotoluene radical cations in the internal energy range 2.0−3.6 eV at 298 K. k_{uni} is the reciprocal of the effective decay time constant of $C_7H_7Br^{+\bullet}$. The theoretical values of k_{uni} decrease in the order ortho > para > meta, over the entire internal energy range and k_{uni} of the *m*-isomer is less than a half k_{uni} of the *o*- and *p*-isomers. The calculated rate−energy curves are also compared with the TRPD[9] and PEPICO[3] data. For all three isomers, the rate−energy curve falls closely to the PEPICO data in the internal range 2.7−3.6 eV but falls below the TRPD data in the internal energy range 2.2−2.7 eV. To see the effect of coupling on the kinetics, we plot the ratio of k_{uni} for each isomer over the average value as a function of internal energy in Figure S2 in the Supporting Information. As the energy increases, the relative

dx.doi.org/10.1021/jp4031442 | J. Phys. Chem. A 2013, 117, 11924−11932

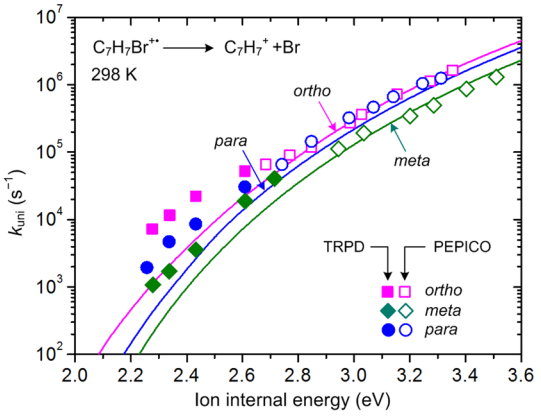

Figure 4. Calculated overall unimolecular dissociation rate constants (lines) for the *o*-, *m*-, and *p*-bromotoluene radical cations in conjunction with the experimental rate constants (symbols) as a function of internal energy at 298 K. Solid symbols denote the rate constants determined by time-resolved photodissociation (TRPD) experiments (ref 9), and open symbols refer to the rate constants determined by photoelectron photoion coincidence (PEPICO) experiments (ref 3).

ratio for the *o*-isomer decreases, whereas those for the *m*- and *p*-isomers increase with the same slope, indicating that the coupling makes the dissociation rates of the three isomers become parallel to each other at high energy although their initial rates significantly vary with energy.

The thermal rate constant $k(T)$ obtained from k_{uni} using eq 5 is plotted against $1/T$ in Figure 5 in the temperature range

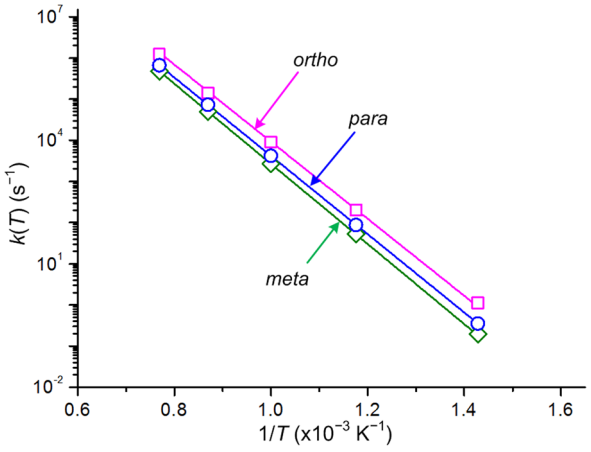

Figure 5. Arrhenius plots of the canonical rate constants for the *o*- (magenta), *m*- (green), and *p*- bromotoluene (blue) radical cations in the temperature range 700−1300 K.

700−1300 K. The values of $k(T)$ decrease in the order ortho > para > meta. Over the entire temperature range, ln $k(T)$ varies linearly with $1/T$. Thus, the Arrhenius equtaion (8) is used to extract the pre-exponential factor A and the activation energy E_a for the coupled unimolecular dissociations of *o*-, *m*-, and *p*-bromotoluene radical cations at 1000 ± 300 K.

$$\ln k(T) = \ln A - \frac{E_a}{RT} \tag{8}$$

R is the gas constant. Values of A and E_a are listed in Table 1. The pre-exponential factor is on the order of 10^{13} s^{-1} and decreases in the order para > ortho > meta. Values of A can be used to calculate entropies of activation at 1000 K ($\Delta S^{\ddagger}$) using eq 9.[23]

$$A = \exp(1)\frac{k_B T}{h}\exp\left(\frac{\Delta S^{\ddagger}}{R}\right) \tag{9}$$

The calculated entropy of activation at 1000 K is −2.8, −2.9, and −2.6 eu for the *o*-, *m*-, and *p*-isomer, respectively. The activation energy is 42, 44, and 44 kcal mol^{-1} for the *o*-, *m*-, and *p*-isomers, respectively. To compare with Arrhenius parameters, we use canonical partition functions to calculate the changes of enthalpy ($\Delta H^{\ddagger}$) and entropy ($\Delta S^{\ddagger}_{Q}$) at 1000 K from the reactant to the highest-lying transition state in the dissociation pathway to the products. Results are included in Table 1. The values of $\Delta H^{\ddagger}$ are almost identical to one another in the benzylium channel: 42 kcal mol^{-1} for the three isomers. In the tropylium channel, the $\Delta H^{\ddagger}$ values increase in the order ortho (47 kcal mol^{-1}) < meta (48 kcal mol^{-1}) < para (51 kcal mol^{-1}), because all three isomers pass through a common highest-lying transition state (TS5) between **5-*o*** and **6**, and the energy level of the reactant decreases in the order ortho > meta > para. $\Delta S^{\ddagger}_{Q}$ values are negative in the range −1.8 to −2.9 eu for the benzylium channel and in the range −2.6 to −3.5 eu for the tropylium channel. Thus, the values of E_a and $\Delta S^{\ddagger}$ obtained from the Arrhenius plot at 1000 ± 300 K are in line with $\Delta H^{\ddagger}$ and $\Delta S^{\ddagger}_{Q}$ calculated at 1000 K for the benzylium channel.

DISCUSSION

In comparison with our previous studies on unimolecular dissociations of chlorotoluene radical cations,[14] the present mechanism includes the [1,2] H-atom migration from **2-*x*** to **3-*x*** (**2-*x*** → **3-*x***) and excludes the [1,3] α-H migration from **1-*x*** to **3-*x*** (**1-*x*** → **3-*x***). At the SCF level of theory, the transition state for [1,2] α-H migration from **1-*x*** to **2-*x*** (**1-*x*** → **2-*x***) lies higher in energy than the transition state for **1-*x*** → **3-*x***. At the B3LYP level, however, the transition state for **1-*x*** → **3-*x*** not only shows a higher barrier height than that for **1-*x*** → **2-*x*** (see

Table 1. Arrhenius Parameters for the Unimolecualr Dissociations of the *o*-, *m*-, and *p*-Bromotoluene Radical Cations and Thermodynamic Parameters for the Benzylium and Tropylium Channels

				to Bz^+		to Tr^+	
reactants	A[a] (×10^{13})	E_a[a] (kcal mol^{-1})	$\Delta S^{\ddagger}$ (eu)[b]	$\Delta H^{\ddagger}$ (kcal mol^{-1})[c]	$\Delta S^{\ddagger}_{Q}$ (eu)[d]	$\Delta H^{\ddagger}$ (kcal mol^{-1})[e]	$\Delta S^{\ddagger}_{Q}$ (eu)[f]
ortho	1.4	42	−2.8	42	−2.9	47	−3.2
meta	1.3	44	−2.9	42	−2.1	48	−3.5
para	1.6	44	−2.6	42	−1.8	51	−2.6

[a]In the temperature range 700−1300 K. [b]From eq 9 at 1000 K. [c]$\Delta H^{\ddagger}$ = H(TS2) − H(**1-*o***), H(TS7) − H(**1-*m***), and H(TS13) − H(**1-*p***) for the *o*-, *m*-, and *p*-isomers, respectively, at 1000 K. [d]$\Delta S^{\ddagger}_{Q}$ = S(TS2) − S(**1-*o***), S(TS7) − S(**1-*m***), and S(TS13) − S(**1-*p***) for the *o*-, *m*-, and *p*-isomers, respectively, at 1000 K. Entropy is calculated using the vibrational and rotational partition functions. [e]$\Delta H^{\ddagger}$ = H(TS5) − H(**1-*x***) (*x* = *o*, *m*, *p*) at 1000 K. [f]$\Delta S^{\ddagger}_{Q}$ = S(TS5) − S(**1-*x***) (*x* = *o*, *m*, *p*) at 1000 K.

dx.doi.org/10.1021/jp4031442 | J. Phys. Chem. A 2013, 117, 11924−11932

Table S1 in the Supporting Information) but also has the same structure as the transition state for **2-*x*** → **3-*x***. This result indicates that the two product channels arise from a common intermediate **2-*x*** rather than from a reactant **1-*x***, thus resolving the controversy over the starting point of the channel splitting. Thus, we replace **1-*x*** → **3-*x*** with **1-*x*** → **2-*x*** → **3-*x*** to take the minimum-energy pathway on the basis of the least action principle, as shown in Scheme 2.

Scheme 2. Consecutive Process of the [1,2] α-Hydrogen Migration from the Reactant 1-*x* to 2-*x* Followed by the [1,2] Hydrogen Migration from 2-*x* to 3-*x* That Is Equivalent to the Direct [1,3] α-Hydrogen Migration from 1-*x* to 3-*x*[a]

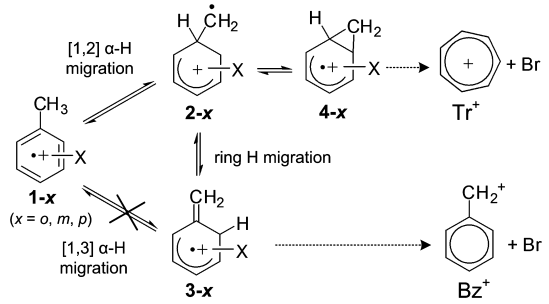

[a]The direct process is excluded in the mechanism because the transition state from **1-*x*** to **3-*x*** is found to be identical to that from **2-*x*** to **3-*x***. Thus, **2-*x*** is a common intermediate for the two product channels.

Hence, the first step at the entrance involves [1,2] α-H migration (**1-*x*** → **2-*x***), which is common to both the benzylium and the tropylium pathways, and the second step is split into two paths, the [1,2] H-atom migration on the ring (**2-*x*** → **3-*x***) toward the benzylium ion and the CH_2 bridging on the ring (**2-*x*** → **4-*x***) toward the tropylium ion. Importantly, the CH_2 migration on the ring (**4-*o*** ↔ **2-*o*** ↔ **4-*m*** ↔ **2-*m*** ↔ **4-*p*** ↔ **2-*p***) can couple the three isomers (Figure 2d) prior to ring expansion. After ring expansion, the [1,2] H-atom migration on the seven-membered ring (**5-*o*** ↔ **5-*m*** ↔ **5-*p***) can also couple the three isomers.

In the cases of the uncoupled reactions presented in our previous report, the decay of the reactant **1-*x*** undergoing two competing pathways to the products was fit to a single-exponential function and the product branching ratio was time-independent. In the present cases of coupled reactions, the decay of $C_7H_7Br^{+\bullet}$ shows a multiexponential behavior with three distinct time zones. In the early time zone, the reaction rate of each isomer appears to be independent from the other isomers, thus exhibiting a fast single-exponential decay. In the intermediate time zone, the decay rate of the initial reactant slows down along with the rise of the other isomers due to coupling. Of the three **1-*x*** species, the globally most stable **1-*p*** is least abundant, whereas **1-*m*** is most abundant after an initial induction period because of the most stable intermediate **3-*m***. In the later time zone, a steady state is reached and all transient **1-*x*** species descend with time constants nearly identical to one another. As a result, the product branching ratio becomes time-dependent, as shown in Figure 3c. Obviously, the unimolecular dissociation kinetics for each isomer is not independent of that of the other ones because the coupling is rather strong, which addresses the issue over the reaction coupling. Thus, the overall kinetics cannot be described by the steady-state approximation.

Theoretical rate constants are in line with the PEPICO data in the high-energy range, but they fall below the TRPD data in the low-energy range. The present calculations significantly underestimate k_{uni} in the low-energy range. This discrepancy between experiment and theory is ascribed to the contribution of the radiative relaxation rate of a hot molecule. The radiative relaxation rate can increase the overall decay rate of an energized molecule and it is getting more important in the energy range where the radiative decay rate is comparable to or faster than the unimolecular dissociation rate. Especially under the conditions of TRPD experiments, where the total pressure was 6×10^{-8} Torr and the ion temperature was 298 K, the radiative decay of the bromotoluene radical cations excited to the internal energy of 2.2−2.7 eV could be very important. The rate−energy curve shown in Figure 4 indicates that the contribution of the radiative relaxation to the overall decay appears to be significant in the energy range where the unimolecular dissociation rate constant is below 10^5 s^{-1}. The rate constant for the radiative relaxation (k_{rad}) is estimated to be on the order of 10^3−10^4 s^{-1} for bromotoluene radical cations having an internal energy of 2.2−2.7 eV at 298 K. This estimate of k_{rad} is somewhat greater than the reported value of 160 s^{-1} for the *p*-iodotoluene radical cation with an internal energy of 2.0 eV at 350−375 K.[6]

Another reason for the discrepancy between experiment and theory might be related to the uncertainties of the potential energy surface. For example, the present level of theory at B3LYP/aug-cc-pVDZ predicts that the tropylium ion is 8.2 kcal mol^{-1} more stable than the benzylium ion. The B3LYP calculations with several split-valence basis sets from 6-31G(d,p) to 6-311G(3df,2p) have predicted the relative energy of 8.1−8.8 kcal mol^{-1}.[13,18] The QCISD(T) calculations with basis sets from 6-31G(d,p) to 6-311G(3df,2p) have yielded 7.2−8.2 kcal mol^{-1}.[16−18] CASSCF(6,7)/6-311G(d,p) and CASMP2/6-311G(d,p) calculations have provided 7.8 and 6.0 kcal mol^{-1}, respectively.[18] Thus, our potential energy surface could have uncertainties of 1−2 kcal mol^{-1} in the energy levels of local minima. Uncertainties are also present in the energy levels of the transition states, where both the electron configuration and the size of basis sets are important. For instance, as we go from SCF to B3LYP with aug-cc-pVDZ basis sets, the highest barrier on the minimum-energy pathway to the products decreases by 0−3 kcal mol^{-1}. Relative energies of local minima and transition states obtained from SCF and B3LYP levels are compared in Table S4 in the Supporting Information. Uncertainties in the energy levels of local minima and transition states would hardly induce any shift in the rate−energy curves in the high-energy region where the PEPICO data were taken but could induce a significant change near the dissociation threshold where the TRPD data were obtained.

Comparison of Arrhenius parameters (E_a and $\Delta S^{\ddagger}$) with the change of enthalpy ($\Delta H^{\ddagger}$) and entropy ($\Delta S^{\ddagger}_{Q}$) provide some insights into the rate-limiting steps in the benzylium channel. For all three isomers, the highest-lying transition state is located between **2-*x*** and **3-*x***, which involves [1,2] H-atom migrations on the six-membered ring. Because the intermediate **2-*x*** results from **1-*x*** through the [1,2] α-H migration, a series of [1,2] H-atom migrations is considered to be the rate-limiting steps. In the case of the *o*-isomer, Arrhenius parameters of E_a = 42 kcal mol^{-1} and $\Delta S^{\ddagger}$ = −2.8 eu are in excellent agreement with thermodynamic values of $\Delta H^{\ddagger}$ = 42 kcal mol^{-1} and $\Delta S^{\ddagger}_{Q}$ = −2.9 eu for the activation of the reactant **1-*o*** to the transition state TS2 between **2-*o*** and **3-*o***. Thus, a series of [1,2] H-atom

dx.doi.org/10.1021/jp4031442 | J. Phys. Chem. A 2013, 117, 11924−11932

migrations comprise the rate-determining steps. For the *m*-isomer, E_a = 44 kcal mol^{-1} and $\Delta S^{\ddagger}$ = −2.9 eu are slightly higher in energy and more negative in entropy than $\Delta H^{\ddagger}$ = 42 kcal mol^{-1} and $\Delta S^{\ddagger}_{Q}$ = −2.1 eu for the rate-limiting consecutive [1,2] H-atom migrations from **1-*m*** to **2-*m*** and to **3-*m*** via TS7. Both the increase in activation energy and the decrease in activation entropy suggest that the extra stability of **3-*m*** plays a significant role in impeding the subsequent [1,2] H-atom migration from **3-*m*** to **7** and diverting the reaction to other exit channels. With the *p*-isomer, E_a = 44 kcal mol^{-1} and $\Delta S^{\ddagger}$ = −2.6 eu are slightly different from $\Delta H^{\ddagger}$ = 42 kcal mol^{-1} and $\Delta S^{\ddagger}_{Q}$ = −1.8 eu for the consecutive [1,2] H-atom migrations from **1-*p*** to **2-*p*** and to **3-*p*** via TS13. The difference between the activation parameters and the thermodynamic values suggests that a series of subsequent [1,2] H-atom migrations from **3-*p*** to **5-*p*** and to **9** reduce the net flux toward the product, thereby increasing the activation energy and further decreasing the activation entropy.

Importantly, Arrhenius parameters (E_a and A) listed in Table 1 can be used in the measurement of the ion temperature of the *o*-, *m*-, and *p*-bromotoluene radical cations from their dissociation yields in the temperature range 700−1300 K, as previously shown in the measurement of the ion temperature from the peptide fragmentation yield.[24]

The values of E_a and $\Delta S^{\ddagger}$ listed in Table 1 cannot be directly compared with the values of E_0 and $\Delta S^{\ddagger}_{exp}$ reported by Kim and Shin,[9] because the latter values are not the Arrhenius parameters for thermal reactions but the adjusting parameters that fit the TRPD and PEPICO rate−energy data, as displayed in Figure 4, to the microcanonical rate−energy curve. The reported E_0 value is 38.3, 41.5, and 41.0 kcal mol^{-1} for the *o*-, *m*-, and *p*-isomers, respectively. Although E_0 values are 3−4 mol^{-1} less than E_a values, both E_0 and E_a decrease in the same order, meta > para > ortho. In contrast, the values of $\Delta S^{\ddagger}_{exp}$ (−9.0, −7.2, and −5.8 eu for the *o*-, *m*-, and *p*-isomers, respectively) are too negative compared to the Arrhenius $\Delta S^{\ddagger}$ values (−2.80, −2.88, and −2.56 eu for the *o*-, *m*-, and *p*-isomers, respectively).

The present kinetic method for the coupled dissociation reactions can be applied to the unimolecular dissociations of alkylbenzene radical cations that involve multiple rearrangement processes. Of the alkylbenzenes, xylene is similar to halotoluene and ethylbenzene is similar to benzyl halide, except for the methyl group replacing the halogen atom. The unimolecular dissociations of the xylene and ethylbenzene radical cations have been studied by both experiments[25,26] and theory.[27,28] Recent PEPICO experiments[25] have shown that the overall dissociation rate of the xylene radical cation is 2 orders of magnitude slower than that of the ethylbenzene radical cation and $\Delta S^{\ddagger}$ is more negative for the xylene radical cation than for the ethylbenzene radical cation. More recent DFT studies[28] have found that the dissociation pathway of the xylene radical cation to the benzylium or tropylium ion involves a series of the H-atom migrations as well as the coupling of *o*-, *m*-, and *p*-isomers through CH_2 migrations, whereas the ethylbenzene radical cation predominantly dissociates to the benzylium ion by the direct C_α−C_β cleavage without multiple rearrangements. Thus, the full kinetic simulation method employed in the present work could provide a better understanding of the coupled multibarrier unimolecular dissociations of the *o*-, *m*-, and *p*-xylene radical cations.

CONCLUSION

The unimolecular dissociations of bromotoluene radical cations proceed to the benzylium product through a series of hydrogen migrations and to the tropylium product through a combination of consecutive hydrogen and methylene migrations before the ring expansion. The two product channels originate from a common intermediate formed by [1,2] α-H migration at the entrance. All three isomers are coupled to one another through methylene migrations prior to the ring expansion and [1,2] H-atom migrations after the ring expansion. As a result of coupling, all three isomers yield the benzylium ion through three exit channels but result in the tropylim ion mostly through the exit channel of the *o*-isomer. Thus, the overall decay of the reactant is multiple-exponential and the product branching ratio becomes time-dependent. Consequently, the steady-state approximation is not valid to describe the kinetics of the coupled unimolecular dissociations of bromotoluene radical cations. Nonetheless, the activation energy and entropy extracted from the Arrhenius plot of thermal dissociation rate constants can be used to measure the ion temperature from the dissociation yield. Further experiments are warranted for direct confirmation of the time dependence of the product branching ratio.

ASSOCIATED CONTENT

Supporting Information

Molecular parameters, such as the total energies, zero-point energies, relative energies, rotational constants, and vibrational frequencies; parameters of the multiexponential fit to the temporal variation of some transient species; comparison of relative energies from HF and B3LYP calculations; plots of the normalized relative abundances of the product ions; plots of the ratio of k_{uni} for each isomer to their sum; full citation of ref 21; formulation of the matrix equation to solve the coupled differential rate equations; evaluation of the product yields originated from four different exit channels. This information is available free of charge via the Internet at http://pubs.acs.org.

AUTHOR INFORMATION

Corresponding Author

*S. K. Shin: e-mail, skshin@postech.ac.kr.

Notes

The authors declare no competing financial interest.

ACKNOWLEDGMENTS

J. Seo acknowledges the postdoctoral support from the Brain Korea 21 program administered by the Ministry of Education, Science and Technology of Korea.

REFERENCES

(1) Dunbar, R. C.; Honovich, J. P.; Asamoto, B. Photodissociation Themochemistry as a Probe of Halotoluene Ion Potential Surfaces. *J. Phys. Chem.* **1988**, *92*, 6935−6939.

(2) Baer, T.; Morrow, J. C.; Shao, J. D.; Olesik, S. Gas-Phase Heats of Formation of $C_7H_7^+$ Isomers: *m*-Tolyl, *p*-Tolyl, and Benzyl Ions. *J. Am. Chem. Soc.* **1988**, *110*, 5633−5638.

(3) Olesik, S.; Baer, T.; Morrow, J. C.; Ridal, J. J.; Buschek, J. M.; Holmes, J. L. Dissociation Dynamics of Halotoluene Ions, Production of Tolyl, Benzyl, and Tropylium ($[C_7H_7]^+$) Ions. *Org. Mass Spectrom.* **1989**, *24*, 1008−1016.

(4) Dunbar, R. C.; Lifshitz, C. Slow Time-Resolved Photodissociation of *p*-Iodotoluene Ion. *J. Chem. Phys.* **1991**, *94*, 3542−3547.

(5) Choe, J. C.; Kim, M. S. Dissociation Dynamics of *m*-Iodotoluene Molecular Ion: Photodissociation and Metastable Ion Decomposition. *Int. J. Mass Spectrom. Ion Processes* **1991**, *107*, 103−126.
(6) Lin, C. Y.; Dunbar, R. C. Time-Resolved Photodissociation Rates and Kinetic Modeling for Unimolecular Dissociation of Iodotoluene Ions. *J. Phys. Chem.* **1994**, *98*, 1369−1375.
(7) Cho, Y. S.; Kim, M. S.; Choe, J. C. Reinvestigation of the Photodissociation Kinetics of *m*-Iodotoluene Molecular Ion. *Int. J. Mass Spectrom. Ion Processes* **1995**, *145*, 187−195.
(8) Shin, S. K.; Han, S. J.; Kim, B. Time-Resolved Photodissociation of *p*-Bromotoluene Ion as a Probe of Ion Internal Energy. *Int. J. Mass Spectrom. Ion Processes* **1996**, *157/158*, 345−355.
(9) Kim, B.; Shin, S. K. Time- and Product-Resolved Photodissociations of Bromotoluene Radical Cations. *J. Chem. Phys.* **1997**, *106*, 1411−1417.
(10) Kim, B.; Shin, S. K. Time-Resolved Photodissociations of Iodotoluene Radical Cations. *J. Phys. Chem. A* **2002**, *106*, 9918−9924.
(11) Shin, S. K.; Kim, B.; Jarek, R. L.; Han, S. J. Product-Resolved Photodissociations of Iodotoluene Radical Cations. *Bull. Korean Chem. Soc.* **2002**, *23*, 267−270.
(12) Kim, S.-J.; Shin, C.-H.; Shin, S. K. Ab Initio Quantum Mechanical Investigation of the Reaction Mechanisms for the Formation of $C_7H_7^+$ from *o*-, *m*-, and *p*-Chlorotoluene Radical Cations. *Mol. Phys.* **2007**, *105*, 2541−2549.
(13) Choe, J. C. Formation of $C_7H_7^+$ From Benzyl Chloride and Chlorotoluene Molecular Ions: A Theoretical Study. *J. Phys. Chem. A* **2008**, *112*, 6190−6197.
(14) Seo, J.; Seo, H.-I.; Kim, S.-J.; Shin, S. K. The Kinetics of Competing Multiple-Barrier Unimolecular Dissociations of *o*-, *m*-, and *p*-Chlorotoluene Radical Cations. *J. Phys. Chem. A* **2008**, *112*, 6877−6883.
(15) Choe, J. C. Dissociation of Bromo- and Iodotoluene Molecular Ions: A Theoretical Study. *Int. J. Mass Spectrom.* **2008**, *278*, 50−58.
(16) Nicolaides, A.; Radom, L. Seven-Membered Ring or Phenyl-Substituted Cation? Relative Stabilities of the Tropylium and Benzyl Cations and Their Silicon Analogs. *J. Am. Chem. Soc.* **1994**, *116*, 9769−9770.
(17) Smith, B. J.; Hall, N. E. G2(MP2, SVP) Study of the Relationship Between the Benzyl and Tropyl Radicals, and Their Cation Analogues. *Chem. Phys. Lett.* **1997**, *279*, 165−171.
(18) Shin, S. K. Relative Stabilities of *Ortho*-, *Meta*-, and *Para*-Tolyl Cations. *Chem. Phys. Lett.* **1997**, *280*, 260−265.
(19) Peng, C.; Ayala, P. Y.; Schlegel, H. B.; Frisch, M. J. Using Redundant Internal Coordinates to Optimize Equilibrium Geometries and Transition States. *J. Comput. Chem.* **1996**, *17*, 49−56.
(20) Sinha, P.; Boesch, S. E.; Gu, C.; Wheeler, R. A.; Wilson, A. K. Harmonic Vibrational Frequencies: Scaling Factors for HF, B3LYP, and MP2 Methods in Combination with Correlation Consistent Basis Sets. *J. Phys. Chem. A* **2004**, *108*, 9213−9217.
(21) Frisch, M. J.; Trucks, G. W.; Schlegel, H. B.; Scuseria, G. E.; Robb, M. A.; Cheeseman, J. R.; Montgomery, J. A., Jr.; Vreven, T.; Kudin, K. N.; Burant, J. C. et al. *Gaussian 03*, Revision B.04; Gaussian, Inc.: Pittsburgh, PA, 2003.
(22) Baer, T.; Hase, W. L. *Unimolecular Reaction Dynamics: Theory and Experiments*; Oxford University Press: New York, 1996.
(23) Houston, P. L. *Chemical Kinetics and Reaction Dynamics*; McGraw-Hill: Boston, 2001.
(24) Seo, J.; Suh, M.-S.; Yoon, H.-J.; Shin, S. K. N-Acylated Dipeptide Tags Enable Precise Measurement of Ion Temperature in Peptide Fragmentation. *J. Phys. Chem. B* **2012**, *116*, 13982−13990.
(25) Malow, M.; Penno, M. P.; Weitzel, K.-M. The Kinetics of Methyl Loss from Ethylbenzene and Xylene Ions: The Tropylium versus Benzylium Story Revisited. *J. Phys. Chem. A* **2003**, *107*, 10625−10630.
(26) Fridgen, T. D.; Troe, J.; Viggiano, A. A.; Midey, A. J.; Williams, S.; McMahon, T. B. Experimental and Theoretical Studies of the Benzylium$^+$/Tropylium$^+$ Ratios after Charge Transfer to Ethylbenzene. *J. Phys. Chem. A* **2004**, *108*, 5600−5609.
(27) Schulze, S.; Paul, A.; Weitzel, K.-M. Formation of $C_7H_7^+$ Ions from Ethylbenzene and *o*-Xylene Ions: Fragmentation versus Isomerization. *Int. J. Mass Spectrom.* **2006**, *252*, 189−196.
(28) Choe, J. C. Isomerization and Dissociation of Ethylbenzene and Xylene Molecular Ions: A DFT Study. *Chem. Phys. Lett.* **2007**, *435*, 39−44.